

Efficient Arbitrary Precision Acceleration for Large Language Models on GPU Tensor Cores

Shaobo Ma¹, Chao Fang¹, Haikuo Shao¹, Zhongfeng Wang^{1,2}

¹School of Electronic Science and Engineering, Nanjing University, Nanjing, China

²School of Integrated Circuits, Sun Yat-sen University, Shenzhen, China
{shaoboma,fantasysee,hkshao}@smail.nju.edu.cn,zfwang@nju.edu.cn

ABSTRACT

Large language models (LLMs) have been widely applied but face challenges in efficient inference. While quantization methods reduce computational demands, ultra-low bit quantization with arbitrary precision is hindered by limited GPU Tensor Core support and inefficient memory management, leading to suboptimal acceleration. To address these challenges, we propose a comprehensive acceleration scheme for arbitrary precision LLMs. At its core, we introduce a novel bipolar-INT data format that facilitates parallel computing and supports symmetric quantization, effectively reducing data redundancy. Building on this, we implement an arbitrary precision matrix multiplication scheme that decomposes and recovers matrices at the bit level, enabling flexible precision while maximizing GPU Tensor Core utilization. Furthermore, we develop an efficient matrix preprocessing method that optimizes data layout for subsequent computations. Finally, we design a data recovery-oriented memory management system that strategically utilizes fast shared memory, significantly enhancing kernel execution speed and minimizing memory access latency. Experimental results demonstrate our approach's effectiveness, with up to 13× speedup in matrix multiplication compared to NVIDIA's CUTLASS. When integrated into LLMs, we achieve up to 6.7× inference acceleration. These improvements significantly enhance LLM inference efficiency, enabling broader and more responsive applications of LLMs.

KEYWORDS

Large Language Model, Inference Acceleration, GPU, Ultra-Low Bit Quantization, Tensor Core

1 INTRODUCTION

In recent years, large language models (LLMs) based on the Transformer [33] architecture have been rapidly developed and gained popularity, with the GPT family [2, 3, 26, 28, 29] being one of the most prominent examples. These models have demonstrated remarkable performance across a wide range of natural language tasks. However, the increasing size and complexity of LLMs pose significant challenges for efficient inference. To address this issue,

various acceleration methods [7, 9, 10, 19, 31, 36] have been proposed, among which model quantization [7, 10, 13, 16, 20, 30, 36] has emerged as a promising approach. By reducing the data bit-width, quantization explicitly decreases memory consumption and computation time while minimizing the impact on the overall model structure and performance.

As quantization methods continue to evolve, the quantization of LLM models has reached ultra-low bit-widths [20, 30], such as 2-bit and 3-bit. However, the mismatch between these advanced quantization methods and the capabilities of mainstream GPU devices leads to several challenges in practical deployment [8, 17, 21], which manifests in the following aspects:

1) Limited data format support in GPU Tensor Cores (TCs). TCs are the key hardware components in modern GPUs for accelerating matrix multiplications (MatMuls), which dominate the operations in LLMs. Starting with the Turing architecture, Nvidia GPU TCs support some low-precision tensor operations, such as INT1 and INT4, and even bit-level operations [18]. However, TCs still lack support for certain data formats that are widely used by ultra-low-bit quantized LLMs, such as INT2 [15] and INT3 [10]. When deploying these models on GPUs, the low-bit quantized data needs to be converted into higher-bit data formats supported by TCs for computation. This data format conversion introduces additional computational overhead, preventing some ultra-low-bit quantized LLMs from achieving optimal inference acceleration on GPU platforms.

2) Inefficient GPU memory management schemes. When deploying LLMs on GPUs, performance bottlenecks arise not only from MatMuls but also from data access. GPUs employ a multi-level memory hierarchy [24], with different levels varying in capacity and bandwidth. Effective memory management significantly impacts data access latency. For example, by carefully coordinating the use of different GPU memory levels, such as texture and shared memory, memory-bound applications can achieve significant speedup up to 14.8×, compared to unoptimized implementations [39]. Consequently, some optimization schemes that focus solely on MatMuls while neglecting the importance of GPU memory management fail to achieve the desired performance improvements in practice and may even result in slower execution times than the original, unoptimized one [4].

To address these challenges, we first propose a novel data format called bipolar-INT, which features a symmetric range and eliminates redundant sign bits, thereby reducing redundancy and facilitating parallel computing. Secondly, to overcome the limited precision support of GPU TCs, we achieve arbitrary precision MatMul through bit-level decomposition and recovery of matrices, saving memory while maintaining flexibility. Next, we introduce an efficient matrix

Permission to make digital or hard copies of all or part of this work for personal or classroom use is granted without fee provided that copies are not made or distributed for profit or commercial advantage and that copies bear this notice and the full citation on the first page. Copyrights for components of this work owned by others than the author(s) must be honored. Abstracting with credit is permitted. To copy otherwise, or republish, to post on servers or to redistribute to lists, requires prior specific permission and/or a fee. Request permissions from permissions@acm.org.

ASPDAC '25, January 20–23, 2025, Tokyo, Japan

© 2025 Copyright held by the owner/author(s). Publication rights licensed to ACM.

ACM ISBN 979-8-4007-0635-6/25/01

<https://doi.org/10.1145/3658617.3697668>

preprocessing method that preprocesses input matrices by decomposing and reassembling them in advance, reducing communication costs and facilitating subsequent computations. Finally, we propose a memory management approach oriented by efficient data recovery, aiming to maximize the use of faster shared memory for tasks originally handled by global memory, greatly enhancing kernel execution speed. Ultimately, compared to NVIDIA’s MatMul acceleration design CUTLASS, our scheme achieves up to a 13× speedup in MatMul and up to a 6.7× inference acceleration when integrated into LLMs.

In summary, the main contributions of this paper are as follows:

- We propose a novel data format called bipolar-INT for efficient arbitrary precision MatMuls, featuring a symmetric range and eliminating redundant sign bits. (Section 3.1)
- We present an innovative design for arbitrary precision MatMuls on GPUs, optimizing memory usage without sacrificing flexibility. (Section 3.2)
- An efficient matrix preprocessing method is designed to reduce communication costs and facilitate subsequent matrix computations. (Section 4.1)
- A hierarchical memory management strategy oriented by efficient data recovery is proposed, which greatly enhances kernel execution speed. (Section 4.2)

2 BACKGROUND

2.1 Ultra-Low Bit Quantized LLMs

The rapid development of LLMs has led to a significant increase in model size and computational complexity, posing challenges for efficient inference. To address this issue, model quantization [7, 10, 22, 37] has emerged as a promising approach, aiming to reduce the computational complexity and memory footprint of LLMs.

Early LLM quantization methods focused on traditional techniques such as FP16 optimization [26] and INT8 quantization. For example, GPT3.INT8() [6] addressed the issue of outliers in LLMs’ quantization by employing mixed-precision computation. However, to further push the performance frontier, more aggressive quantization methods with lower bit-widths have been proposed, such as QLoRA [7] with 4-bit, GPTQ [10] with 3–4 bit, SqueezeLLM [16] with 3-bit, TSLD [15] with ternary, and OneBit [37] with binary quantization for LLMs. Despite the promising results achieved by these ultra-low bit quantization methods, their optimal inference performance on GPUs has been hindered by the lack of suitable data formats supported by GPU hardware. This limitation calls for efficient acceleration designs that can bridge the gap between the quantization methods and the available GPU hardware capabilities, enabling LLMs to fully benefit from the reduced precision and computational complexity offered by ultra-low bit quantization.

2.2 GPU Hierarchy and Tensor Core

GPUs have become essential for AI workloads due to their highly parallel computing structure. Modern GPUs feature a multi-level memory hierarchy, including global memory, shared memory, registers, and caches (L1 and L2), each with different sizes and access speeds. Global memory, the largest and slowest, is accessible by all threads, while shared memory, though smaller, is faster and accessible within a block, reducing latency. Registers, the fastest

memory component, store frequently accessed variables for individual threads. L1 and L2 caches further expedite data access, with L1 being faster and L2 larger and shared among cores [1, 14, 23].

To accelerate deep learning workloads, NVIDIA introduced TCs in their GPUs. Optimized for MatMuls, a critical operation in LLMs, TCs leverage the massive parallelism of GPUs to significantly improve computational efficiency and inference performance [1, 14, 23, 25, 35]. However, while TCs support low-precision data formats like INT1, INT4, and INT8, they lack support for efficient arbitrary precision operations. This limitation hinders the efficient acceleration of ultra-low bit quantized LLMs, necessitating a novel acceleration scheme that fully utilizes TCs to perform quantized LLMs with arbitrary precision [8].

2.3 Arbitrary Precision Acceleration Schemes

Arbitrary precision acceleration schemes for data formats lower than INT8 have been extensively studied [5, 8, 11, 12, 17, 18, 27, 32, 34, 38, 40] to optimize inference performance and maintain model accuracy for diverse application requirements. In addition to the commonly supported precisions on modern GPUs (e.g., INT1, INT4), these designs often incorporate a broader range of precisions such as INT2, INT3. Among these schemes, APNN-TC [8] supports arbitrary precision, HAQ [34] employs 1–8 bits, while BSTC [17] and BTC [18] focus on 1-bit precision. These works designed MatMul kernels supporting various precisions and integrated them into quantized neural networks to enhance performance. However, they have limitations in terms of incomplete support for arbitrary precision, as exemplified by APNN-TC not supporting W3A4, and suboptimal performance for large matrix parameters due to unsuitable data formats and inefficient GPU memory management. To address these issues, our work aims to identify a more suitable data format for arbitrary precision MatMul, implement kernel support for true arbitrary precision, and further optimize MatMul performance through improved memory scheduling.

3 ARBITRARY PRECISION MATMUL

This section presents the arbitrary precision integers MatMul framework implemented on TCs. First, we introduce an efficient data format, namely bipolar-INT, and demonstrate its advantages over traditional signed and unsigned integers for TCs’ deployment. Next, we propose a bit-wise MatMul decomposition method to separate the operands bit by bit based on our bipolar-INT, utilizing the bit-wise computing kernel supported by TCs, and further develop the data recovery dataflow.

3.1 Bipolar-INT Data Format

We introduce a novel and efficient data format called bipolar-INT for arbitrary precision MatMul computations. Compared to original signed and unsigned integers, bipolar-INT is more suitable for LLM quantization and parallel computing due to its symmetric range and unified operations, making it particularly advantageous for deployment on TCs.

As shown in Fig. 1, the key difference between bipolar-INT and traditional integers lies in the interpretation of each bit. In traditional integers, each bit except the sign bit is valued as 0 or 1,

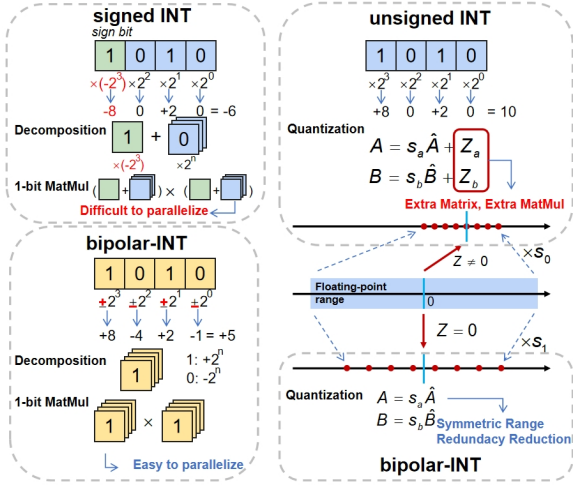


Figure 1: Comparison between bipolar-INT and traditional integers. Bipolar-INT is well-suited for TCs’ parallel computing due to its symmetric quantization and unified operations.

whereas in bipolar-INT, the "0" is interpreted as "-1" in calculations, allowing each bit to be either -1 or 1. Specifically, for an n-bit bipolar-INT data $x = x^{(n-1)}, \dots, x^{(1)}, x^{(0)}$, its decimal value can be obtained by

$$(x)_D = \sum_{i=0}^{n-1} (2x^{(i)} - 1) \cdot 2^i. \quad (1)$$

For signed INT quantization, as illustrated in Fig. 1, due to the use of two’s complement arithmetic, the sign of the MSB matrix after decomposition is opposite to the signs of the other bits. This requires separate handling during MatMul and matrix reconstruction, which is highly unfavorable for the parallel computation of single-bit matrices at each bit. Similarly, for unsigned INT quantization, the presence of an additional zero-point offset introduces extra multiply-accumulate operations during MatMul, which is detrimental to the optimization of MatMul.

Moreover, for binary quantized neural networks, weights (W) are often quantized to values of either -1 and 1, which are encoded as 1-bit 0 and 1, respectively. If the feature matrix X is quantized to (0,1) with its decimal value also being (0,1), then the MatMul of W and X will be inconsistent during computation. Conventional methods like APNN-TC[8] introduce an additional all-ones matrix $J = [1, 1]$ to tackle this problem. The matrix W is decoded as $\hat{W} = [0, 1]$, which relates to its actual value by $W = 2\hat{W} - J$. Thus, the MatMul becomes $WX = 2\hat{W}X - JX$, which not only introduces an additional matrix J occupying memory, but also introduces an extra MatMul operation JX . In contrast, the binary quantized W aligns perfectly with our 1-bit bipolar-INT format. Therefore, when using bipolar-INT for MatMuls in binary quantized neural networks, the feature matrix X is also quantized using bipolar-INT, without introducing additional matrices or MatMuls for precise computation.

3.2 Bit-Wise MatMul Reconstitution

A bit-wise MatMul reconstitution method is further proposed based on our bipolar-INT format. This method consists of three main

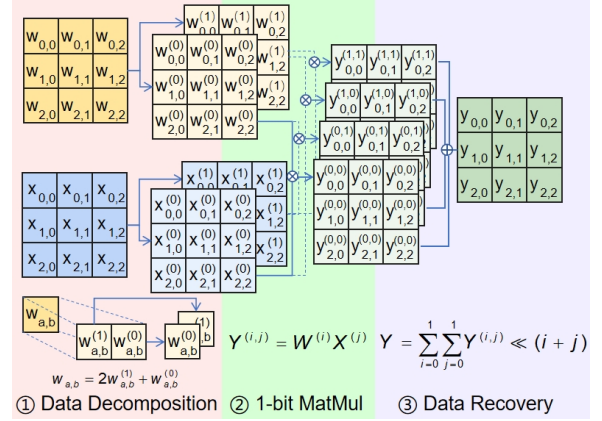


Figure 2: Illustration of the decomposition and recovery process for bipolar-INT MatMuls. Here matrices W and X are both 2-bit, which can be extended to arbitrary bit widths.

steps: data decomposition, 1-bit MatMul, and data recovery. Fig. 2 illustrates the complete computation process of arbitrary precision MatMul using our proposed method. In this example, we consider a MatMul operation involving 2-bit matrices W and X , ultimately calculating a 32-bit output $Y = WX$.

The data decomposition step involves separating the operands bit by bit, enabling the utilization of the bit-wise computing kernel supported by TCs. Specifically, W and X are decomposed into two matrices each, denoted as $W^{(i)}$ and $X^{(j)}$, respectively. After the data decomposition, pairwise 1-bit MatMul operations are performed on the decomposed operands. Nvidia GPUs support the selection of either AND or XOR logic for 1-bit MatMul operations within TCs. By computing the pairwise MatMul of $W^{(i)}$ and $X^{(j)}$, we obtain a 32-bit intermediate result matrix $Y^{(i,j)}$ for each pair of bits. To reconstruct the final result from the intermediate bit-wise computations, a data recovery dataflow is employed. This step involves reconstructing the output matrix Y from the intermediate results $Y^{(i,j)}$ by shifting each $Y^{(i,j)}$ based on its corresponding bit positions (i, j) and then summing up all the shifted matrices.

Although the example in Fig. 2 involves 2-bit matrices, the same principles can be extended to arbitrary bit widths. Our bit-wise MatMul decomposition method, based on the bipolar-INT format, effectively utilizes the bit-wise computing capabilities of TCs, providing a flexible and efficient solution for arbitrary precision MatMul operations.

4 GPU MEMORY SCHEDULING

This section focuses on how to efficiently transfer data between different levels of the memory hierarchy in the arbitrary precision MatMul kernel to maximize processing speed.

4.1 Matrix Decomposition and Reassembly

We present a matrix decomposition and reassembly strategy to efficiently transfer data between different levels of the memory hierarchy in the arbitrary precision MatMul kernel. This strategy

aims to reduce memory access redundancy and maximize data transfer speed by preprocessing the original n -bit INT matrix.

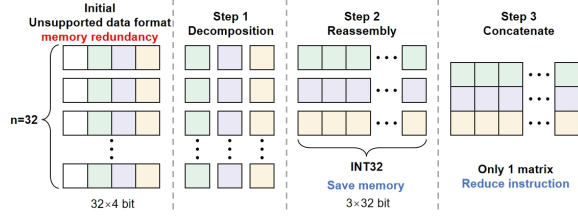


Figure 3: Procedure of matrix decomposition and reassembly to save GPU's memory and data transfer instructions.

As shown in Fig. 3, GPUs support more precisions than TCs when accessing memory, but they still do not support all possible precisions. For example, a 3-bit INT type does not have a suitable storage format and must be stored using a wider data format (such as 4-bit or 8-bit), introducing redundant memory access overhead. Moreover, when the amount of data to be accessed is large, not only the storage precision support but also the suitability of the corresponding data format for data transfer must be considered.

To address these issues, our strategy involves three steps, as illustrated in Fig. 3. In Step 1, we perform 1-bit decomposition on the original matrix, breaking down each bit and regrouping them with corresponding bits from other data to form n 1-bit matrices. This step circumvents the issue of unsuitable data formats and eliminates memory redundancy caused by the lack of appropriate data formats. Next, in Step 2, we reassemble the decomposed data using 32-bit unsigned INTs. This step ensures that the input data aligns with the GPU's native support, thereby enhancing data transfer speed. Finally, in Step 3, we sequentially concatenate the processed n matrices into a single matrix. This step not only further conserves memory but also simplifies n data transfer instructions into a single instruction. Although the amount of data transferred remains the same, this concatenation improves data transfer speed and saves storage space. By following these steps, our matrix decomposition and reassembly strategy effectively reduces memory access redundancy and maximizes data transfer speed in the arbitrary precision MatMul kernel.

4.2 Recovery-Oriented Memory Scheduling

A recovery-oriented memory scheduling strategy is proposed to optimize data transfer and memory access in the arbitrary precision MatMul kernel on GPUs by performing the matrix recovery process in shared memory or fragments, thereby reducing global memory access and computation, and further accelerating the kernel's computation speed.

As shown in Fig. 4, when implementing the arbitrary precision MatMul described in Sec. 3 on a GPU, we perform 1-bit MatMul on the decomposed matrices to obtain intermediate result matrices. These intermediate result matrices are then shifted and summed to get the final result. In a naive approach, each streaming multiprocessor (SM) directly multiplies a pair of 1-bit matrices decomposed from the weights and features, and the MatMul result is directly returned to global memory for recovery. However, this design leads

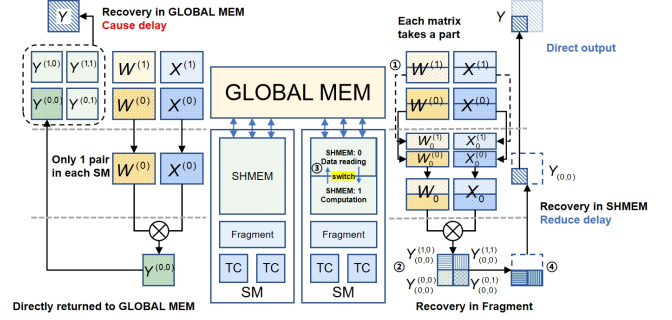


Figure 4: Recovery-oriented memory scheduling strategy for arbitrary precision MatMul on GPUs, leveraging shared memory and fragments to reduce global memory access and accelerate computation.

to each SM obtaining at most one intermediate result matrix, forcing the final matrix recovery to be performed in the slower global memory. This step introduces significant delays because accessing and processing data in global memory is much slower compared to shared memory.

To address this issue, our recovery-oriented memory scheduling strategy aims to compute all intermediate result matrices within a single SM, as shown in ① of Fig. 4. This requires each SM to compute all bitwise combinations of the weight and feature matrices. To efficiently manage shared memory, given its limited size, we divide the output matrix into blocks of size $b_m \times b_n$, with each SM responsible for computing the data within one block. If the number of blocks exceeds the number of SMs, the SMs are iteratively called to perform the computations.

Due to the insufficient size of shared memory, the dimension K needs to be partitioned. Each time, the SM only reads data from two matrices of size $n_{w,x} b_m \times b_k$, and the results of each computation are accumulated over K/b_k iterations to produce the complete output value. In shared memory, the input weight and feature matrices of different bits are concatenated into two matrices and input into the Fragment to call the TC to perform 1-bit matrix multiplication. The resulting $n_w b_m \times n_x b_n$ matrix contains all the data needed to recover a $b_m \times b_n$ output block, as shown in ② of Fig. 4. By sending these data back to shared memory for data recovery, we can obtain part of the final output directly, without involving global memory in the computation.

To hide the data transfer latency from global memory to shared memory, we allocate two blocks of shared memory of the same size, as shown in ③ of Fig. 4. While one block is responsible for computation, the other block reads the next set of data. They then alternate in this manner, effectively overlapping data transfer and computation. Furthermore, to increase data reuse and reduce latency, we allow each Fragment to read the weight matrix of the same bit and all bits of the feature matrix, calculating all intermediate results corresponding to this bit of the weight matrix, as shown in ④ of Fig. 4. This way, we can perform the feature part of the data recovery in the Fragment, leaving the weight part of the recovery for shared memory computation.

By employing this recovery-oriented memory scheduling strategy, we significantly reduce the memory access and computation in global memory, effectively leveraging the faster shared memory and fragments to accelerate the arbitrary precision MatMul kernel on GPUs.

5 EXPERIMENTAL RESULTS

In this section, we evaluate the performance of our arbitrary precision acceleration method for LLMs. Our experiments are conducted on an NVIDIA RTX 3090 GPU within an Ubuntu 18.04 system, using CUDA-11.8 and CUTLASS-2.11. The evaluation is divided into two main parts: (1) an assessment of our arbitrary precision MatMul kernels, and (2) an analysis of its impact on LLM inference performance. Through these experiments, we aim to demonstrate the effectiveness of our approach in accelerating LLM computations across different precision levels.

5.1 Arbitrary Precision Kernel Evaluation

In this subsection, we evaluate our arbitrary precision MatMul kernel design on both square and LLM-specific MatMul tasks, validating the effectiveness of our redundancy reduction and memory management techniques. We compare our designs, including W1A2 (1-bit weights, 2-bit activations), W2A2, and W3A4, with standard FP32 and FP16 MatMuls. We then benchmark against NVIDIA’s Tensor Cores-accelerated ultra-low bit MatMul (CUTLASS INT1 and CUTLASS INT4) to showcase our superior computational performance when using the same TCs. Finally, we compare with other TC-based MatMul acceleration techniques, such as APNN-TC [8], BSTC [17], and BTC [18], to demonstrate the performance advantages of our work in low-bit arbitrary precision acceleration.

Table 1: Arbitrary precision kernel performance in comparison with FP and CUTLASS towards large square MatMuls.

M/N/K	1k/1k/1k		2k/2k/2k		4k/4k/4k	
	Latency	Speedup	Latency	Speedup	Latency	Speedup
FP32	121us	1.00×	779us	1.00×	5690us	1.00×
FP16	44.2us	2.73×	263us	2.96×	1960us	2.90×
CUTLASS INT4	15.8us	7.61×	66.5us	11.7×	386us	14.7×
CUTLASS INT1	9.3us	13.0×	36.9us	21.1×	161us	35.3×
W3A4 (ours)	12.4us	9.74×	50.4us	15.4×	184us	31.0×
W2A2 (ours)	8.7us	13.9×	18.1us	43.0×	46.5us	122×
W1A2 (ours)	9.0us	13.4×	11.7us	66.4×	29.5us	193×

5.1.1 Square MatMul Performance. To demonstrate the computational performance of our proposed MatMul design, we first evaluated its speed on square matrices of various sizes. Table 1 presents the comparison of our work against PyTorch floating-point MatMul and CUTLASS for large MatMuls. The reported latency represents the mean execution time over 1000 iterations, and the speedup is calculated relative to FP32 MatMul under identical conditions.

Compared to FP32 and FP16, our MatMul design shows increasing speedup as matrix size grows. For 4k×4k matrices, our W1A2 configuration achieves a remarkable 193× speedup over FP32 and about 70× over FP16. When compared to CUTLASS, which is limited to int1 and int4 precisions due to TC constraints, our design demonstrates superior performance. For 4k×4k matrices, our W1A2 configuration outperforms CUTLASS INT4 by more than 13×. Notably, both our W1A2 and W2A2 configurations surpass CUTLASS

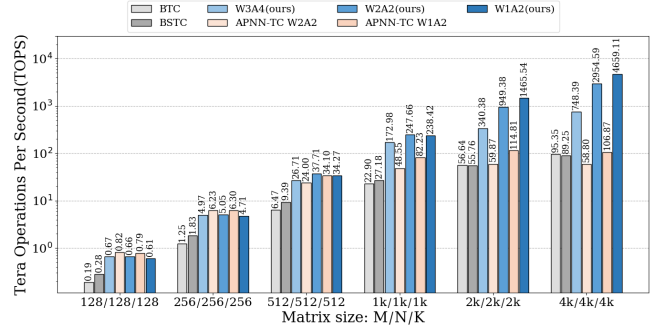


Figure 5: Comparison of throughput between our work and other methods in the context of square MatMuls.

INT1 in performance, despite not having a bit-width advantage. Our W1A2 configuration is 5.5× faster than CUTLASS INT1, while our W2A2 configuration is 3.5× faster. Even our W3A4 configuration, which has a significantly wider bit-width, approaches CUTLASS INT1 performance, achieving approximately 88% of its speed.

Fig. 5 illustrates the performance comparison of our work with other approaches on square matrices from 128×128 to 4k×4k, using Tera Operations Per Second (TOPS) as the metric. Note that APNN-TC is compared only with W1A2 and W2A2 configurations due to its limited precision support.

While APNN-TC slightly outperforms our design for smaller matrices, our approach shows significant advantages for matrices 1k×1k and larger, with our W1A2 and W2A2 configurations achieving 44× and 50× speedups, respectively. This is particularly relevant for LLMs, where large matrix operations are more common. Furthermore, our design offers true arbitrary precision support, including configurations like W3A2 and W3A4, which APNN-TC cannot handle. This demonstrates not only superior performance but also greater flexibility, especially beneficial for the diverse computational needs of LLMs.

Table 2: Arbitrary precision kernel performance in comparison with FP and CUTLASS towards MatMuls in Llama2-7B.

M/N/K	1k/4k/4k		1k/10.5k/4k		1k/4k/10.5k	
	Latency	Speedup	Latency	Speedup	Latency	Speedup
FP32	3.12ms	1.00×	8.21ms	1.00×	8.36ms	1.00×
FP16	1.07ms	2.91×	1.47ms	5.58×	1.58ms	5.30×
CUTLASS INT4	0.238ms	13.1×	0.574ms	14.3×	0.548ms	15.3×
CUTLASS INT1	0.097ms	32.1×	0.255ms	32.2×	0.188ms	44.6×
W3A4 (ours)	0.194ms	16.1×	0.523ms	15.7×	0.540ms	15.5×
W2A2 (ours)	0.059ms	53.2×	0.143ms	57.6×	0.165ms	50.7×
W1A2 (ours)	0.034ms	91.2×	0.084ms	98.1×	0.082ms	102×

5.1.2 LLM-specific MatMul Performance. To more accurately reflect the computational demands of LLMs, we evaluate our MatMul designs on non-square matrices commonly found in these models. We extracted the MatMul parameters from each layer of the Llama2-7B model, providing a real-world benchmark for our evaluation.

Table 2 presents the performance comparison for the three most computationally intensive MatMul operations in Llama2-7B. These operations have the largest number of parameters and the greatest impact on inference time. The reported latency represents the mean

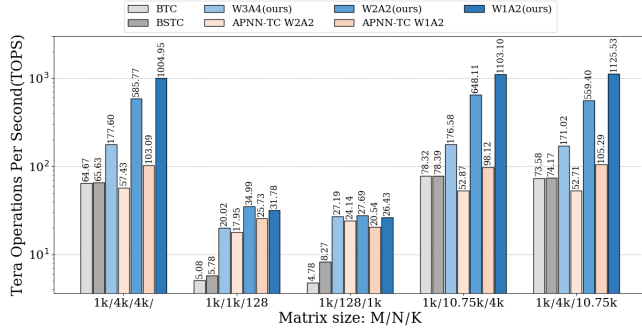


Figure 6: Comparison of throughput between our work and other methods for typical MatMuls from LLMs.

execution time over 1000 iterations, and the speedup is calculated relative to FP32 MatMul under identical conditions.

Our results show that while the acceleration effect slightly decreases for non-square matrices compared to square matrices, our approach still demonstrates outstanding performance. For instance, our W1A2 configuration achieves speedups of 91.2x, 98.1x, and 102x for the three matrix sizes tested, significantly outperforming both FP16 and CUTLASS implementations. Notably, our W1A2 and W2A2 configurations surpass CUTLASS INT1 despite its bit-width advantage, while our W3A4 configuration outperforms CUTLASS INT4. This superior performance can be attributed to our matrix-splitting strategy that minimizes data redundancy and our efficient memory management scheme.

Fig. 6 illustrates the performance comparison across all MatMul sizes in Llama-7B, using TOPS as the metric. When compared to APNN-TC, our design shows similar performance for smaller matrices (e.g., 1kx1kx128). However, for larger matrices more common in LLMs (e.g., 1kx10.75kx4k), our approach achieves over 10x speedup compared to APNN-TC. This disparity is due to our design being optimized specifically for the large matrix computations prevalent in LLMs, whereas APNN-TC’s shared memory allocation and GPU thread scheduling are more suitable for smaller MatMul operations. In summary, our MatMul kernel design demonstrates significant performance advantages in LLM-specific scenarios, particularly for larger, non-square matrices that dominate LLM computations. This makes our approach particularly well-suited for accelerating LLM inference tasks.

5.2 Arbitrary Precision LLM Evaluation

Efficient inference of large language models (LLMs) is crucial for their practical deployment. We evaluate our arbitrary precision MatMul design in ultra-low bit quantized LLMs to demonstrate its effectiveness in accelerating real-world LLM inference.

We focus on three widely studied LLMs: Llama2-7B, OPT-6.7B, and BLOOM-7B. By replacing their standard MatMul operations with our arbitrary precision MatMul kernel, we seek to quantify the performance gains across different model architectures. Our comparison encompasses several state-of-the-art methods: half-precision (FP16) models running on PyTorch, QLoRA [7], GPTQ [10],

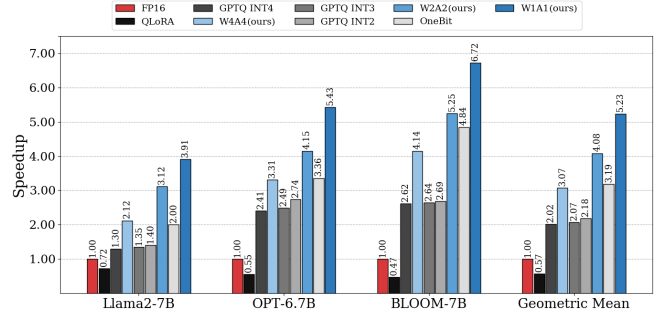


Figure 7: Inference speedup through different quantization frameworks for various LLMs (using FP16 as the baseline).

and OneBit [37]. To ensure a fair comparison, we align our design configurations with these methods: W1A1 for OneBit models, W2A2 for 2-bit quantized GPTQ models, and W4A4 for 4-bit quantized GPTQ models.

Fig. 7 presents the inference speedup for various quantization methods across the three LLMs, using FP16 as the baseline. The results reveal that our work achieves superior acceleration compared to CUTLASS under equivalent bit-width configurations, demonstrating up to nearly 2x speedup. Moreover, when compared to PyTorch’s FP16 implementation, our approach exhibits an impressive 6x speedup. Our analysis indicates that while QLoRA excels in reducing memory usage, its inference speed is compromised due to the necessary precision restoration step. GPTQ, despite offering 2-4 bit quantization, faces limitations imposed by GPU TC precision support. Its reliance on CUTLASS 4-bit as the kernel leads to efficiency trade-offs and suboptimal performance improvements. In contrast, our MatMul scheme demonstrates a 1.2-2x faster model inference speed compared to OneBit (W1A1), attributable to our more efficient memory scheduling.

6 CONCLUSIONS

In this paper, we present a comprehensive scheme to accelerate inference of ultra-low bit quantized large language models (LLMs) on GPU. We first introduce a data format called bipolar-INT, which is suitable for symmetric quantization and conducive to parallel computation. On top of bipolar-INT, we propose an INT MatMul method applicable to arbitrary precision and design an efficient memory management system. Our evaluations demonstrate significant performance gains in both MatMul operations and LLM inference. For MatMul, our implementation achieves a 5.45x speedup compared to Nvidia’s CUTLASS and up to 43x speedup over existing solutions. In LLM inference, our approach yields 3.9-6.7x speedup over FP16 models and 1.2-2x speedup compared to ultra-low bit quantized models using CUTLASS as the kernel.

ACKNOWLEDGMENTS

This work was supported in part by the National Key R&D Program of China under Grant 2022YFB4400600 and in part by the Postgraduate Research & Practice Innovation Program of Jiangsu Province under Grant KYCX24_0149.

REFERENCES

- [1] Hamdy Abdelkhalik, Yehia Arafa, Nandakishore Santhi, and Abdel-Hameed A Badawy. 2022. Demystifying the nvidia ampere architecture through microbenchmarking and instruction-level analysis. In *2022 IEEE High Performance Extreme Computing Conference (HPEC)*. IEEE, 1–8.
- [2] Josh Achiam, Steven Adler, Sandhini Agarwal, Lama Ahmad, Ilge Akkaya, Florencia Leoni Aleman, Diogo Almeida, Janko Altmenschmidt, Sam Altman, Shyamal Anadkat, et al. 2023. Gpt-4 technical report. *arXiv preprint arXiv:2303.08774* (2023).
- [3] Tom Brown, Benjamin Mann, Nick Ryder, Melanie Subbiah, Jared D Kaplan, Prafulla Dhariwal, Arvind Neelakantan, Pranav Shyam, Girish Sastry, Amanda Askell, et al. 2020. Language models are few-shot learners. *Advances in neural information processing systems* 33 (2020), 1877–1901.
- [4] Weiduo Chen, Xiaoshe Dong, Xinhang Chen, Song Liu, Qin Xia, and Qiang Wang. 2023. pommDNN: Performance optimal GPU memory management for deep neural network training. *Future Generation Computer Systems* (2023).
- [5] Matthieu Courbariaux, Yoshua Bengio, and Jean-Pierre David. 2015. Binaryconnect: Training deep neural networks with binary weights during propagations. *Advances in neural information processing systems* 28 (2015).
- [6] Tim Dettmers, Mike Lewis, Younes Belkada, and Luke Zettlemoyer. 2022. Gpt3.int8(): 8-bit matrix multiplication for transformers at scale. *Advances in Neural Information Processing Systems* 35 (2022), 30318–30332.
- [7] Tim Dettmers, Artidoro Pagnoni, Ari Holtzman, and Luke Zettlemoyer. 2024. Qlora: Efficient finetuning of quantized llms. *Advances in Neural Information Processing Systems* 36 (2024).
- [8] Boyuan Feng, Yuke Wang, Tong Geng, Ang Li, and Yufei Ding. 2021. Apnn-tc: Accelerating arbitrary precision neural networks on ampere gpu tensor cores. In *Proceedings of the international conference for high performance computing, networking, storage and analysis*. 1–13.
- [9] Elias Frantar and Dan Alistarh. 2023. SparseGPT: Massive Language Models Can Be Accurately Pruned in One-Shot.(2023). URL <https://arxiv.org/abs/2301.00774> (2023).
- [10] Elias Frantar, Saleh Ashkboos, Torsten Hoefler, and Dan Alistarh. 2022. Gptq: Accurate post-training quantization for generative pre-trained transformers. *arXiv preprint arXiv:2210.17323* (2022).
- [11] Tong Geng, Ang Li, Tianqi Wang, Chunshu Wu, Yanfei Li, Runbin Shi, Wei Wu, and Martin Herbordt. 2020. O3BNN-R: An out-of-order architecture for high-performance and regularized BNN inference. *IEEE Transactions on parallel and distributed systems* 32, 1 (2020), 199–213.
- [12] Song Han, Huizi Mao, and William J Dally. 2015. Deep compression: Compressing deep neural networks with pruning, trained quantization and Huffman coding. *arXiv preprint arXiv:1510.00149* (2015).
- [13] Longwei Huang, Chao Fang, Qiong Li, Jun Lin, and Zhongfeng Wang. 2024. A Precision-Scalable RISC-V DNN Processor with On-Device Learning Capability at the Extreme Edge. In *2024 29th Asia and South Pacific Design Automation Conference (ASP-DAC)*. IEEE, 927–932.
- [14] Zhe Jia, Marco Maggioni, Jeffrey Smith, and Daniele Paolo Scarpazza. 2019. Dissecting the nvidia turing t4 gpu via microbenchmarking. *arXiv preprint arXiv:1903.07486* (2019).
- [15] Minsoo Kim, Sihwa Lee, Janghwan Lee, Sukjin Hong, Du-Seong Chang, Wonyong Sung, and Jungwook Choi. 2024. Token-scaled logit distillation for ternary weight generative language models. *Advances in Neural Information Processing Systems* 36 (2024).
- [16] Sehoon Kim, Coleman Hooper, Amir Gholami, Zhen Dong, Xiuyu Li, Sheng Shen, Michael W Mahoney, and Kurt Keutzer. 2023. SqueezeLLM: Dense-and-sparse quantization. *arXiv preprint arXiv:2306.07629* (2023).
- [17] Ang Li, Tong Geng, Tianqi Wang, Martin Herbordt, Shuaiwen Leon Song, and Kevin Barker. 2019. BSTC: A novel binarized-soft-tensor-core design for accelerating bit-based approximated neural nets. In *Proceedings of the international conference for high performance computing, networking, storage and analysis*. 1–30.
- [18] Ang Li and Simon Su. 2020. Accelerating binarized neural networks via bit-tensor-cores in turing gpus. *IEEE Transactions on Parallel and Distributed Systems* 32, 7 (2020), 1878–1891.
- [19] Shiyang Li, Jianshu Chen, Yelong Shen, Zhiyu Chen, Xinlu Zhang, Zekun Li, Hong Wang, Jing Qian, Baolin Peng, Yi Mao, et al. 2022. Explanations from large language models make small reasoners better. *arXiv preprint arXiv:2210.06726* (2022).
- [20] Ji Lin, Jiaming Tang, Haotian Tang, Shang Yang, Wei-Ming Chen, Wei-Chen Wang, Guangxuan Xiao, Xingyu Dang, Chuang Gan, and Song Han. 2024. AWQ: Activation-aware Weight Quantization for On-Device LLM Compression and Acceleration. *Proceedings of Machine Learning and Systems* 6 (2024), 87–100.
- [21] Yujun Lin, Haotian Tang, Shang Yang, Zhekai Zhang, Guangxuan Xiao, Chuang Gan, and Song Han. 2024. Qserve: W4a8kv4 quantization and system co-design for efficient llm serving. *arXiv preprint arXiv:2405.04532* (2024).
- [22] Zechun Liu, Barlas Oguz, Changsheng Zhao, Ernie Chang, Pierre Stock, Yashar Mehdad, Yangyang Shi, Raghuraman Krishnamoorthi, and Vikas Chandra. 2023. Llm-qat: Data-free quantization aware training for large language models. *arXiv preprint arXiv:2305.17888* (2023).
- [23] Weile Luo, Ruibo Fan, Zeyu Li, Dayou Du, Qiang Wang, and Xiaowen Chu. 2024. Benchmarking and dissecting the nvidia hopper gpu architecture. *arXiv preprint arXiv:2402.13499* (2024).
- [24] Xinxi Mei and Xiaowen Chu. 2016. Dissecting GPU memory hierarchy through microbenchmarking. *IEEE Transactions on Parallel and Distributed Systems* 28, 1 (2016), 72–86.
- [25] Hiroyuki Ootomo and Rio Yokota. 2023. Reducing shared memory footprint to leverage high throughput on Tensor Cores and its flexible API extension library. In *Proceedings of the International Conference on High Performance Computing in Asia-Pacific Region*. 1–8.
- [26] Long Ouyang, Jeffrey Wu, Xu Jiang, Diogo Almeida, Carroll Wainwright, Pamela Mishkin, Chong Zhang, Sandhini Agarwal, Katarina Slama, Alex Ray, et al. 2022. Training language models to follow instructions with human feedback. *Advances in neural information processing systems* 35 (2022), 27730–27744.
- [27] Eunhyeok Park, Dongyoung Kim, and Sungjoo Yoo. 2018. Energy-efficient neural network accelerator based on outlier-aware low-precision computation. In *2018 ACM/IEEE 45th Annual International Symposium on Computer Architecture (ISCA)*. IEEE, 688–698.
- [28] Alec Radford, Karthik Narasimhan, Tim Salimans, Ilya Sutskever, et al. 2018. Improving language understanding by generative pre-training. (2018).
- [29] Alec Radford, Jeffrey Wu, Rewon Child, David Luan, Dario Amodei, Ilya Sutskever, et al. 2019. Language models are unsupervised multitask learners. *OpenAI blog* 1, 8 (2019), 9.
- [30] Wenqi Shao, Mengzhao Chen, Zhaoyang Zhang, Peng Xu, Lirui Zhao, Zhiqian Li, Kaipeng Zhang, Peng Gao, Yu Qiao, and Ping Luo. 2024. OmniQuant: Omnidirectionally Calibrated Quantization for Large Language Models. In *The Twelfth International Conference on Learning Representations (ICLR)*.
- [31] Mingjie Sun, Zhuang Liu, Anna Bair, and J Zico Kolter. 2023. A simple and effective pruning approach for large language models. *arXiv preprint arXiv:2306.11695* (2023).
- [32] Jiayi Tian, Chao Fang, Haonan Wang, and Zhongfeng Wang. 2023. BEBERT: Efficient and robust binary ensemble BERT. In *ICASSP 2023-2023 IEEE International Conference on Acoustics, Speech and Signal Processing (ICASSP)*. IEEE, 1–5.
- [33] Ashish Vaswani, Noam Shazeer, Niki Parmar, Jakob Uszkoreit, Llion Jones, Aidan N Gomez, Łukasz Kaiser, and Illia Polosukhin. 2017. Attention is all you need. *Advances in neural information processing systems* 30 (2017).
- [34] Kuan Wang, Zhijian Liu, Yujun Lin, Ji Lin, and Song Han. 2019. Haq: Hardware-aware automated quantization with mixed precision. In *Proceedings of the IEEE/CVF conference on computer vision and pattern recognition*. 8612–8620.
- [35] Yuke Wang, Boyuan Feng, Zheng Wang, Guyue Huang, and Yufei Ding. 2023. {TC-GNN}: Bridging Sparse {GNN} Computation and Dense Tensor Cores on {GPUs}. In *2023 USENIX Annual Technical Conference (USENIX ATC 23)*. 149–164.
- [36] Guangxuan Xiao, Ji Lin, Mickael Seznec, Hao Wu, Julien Demouth, and Song Han. 2023. Smoothquant: Accurate and efficient post-training quantization for large language models. In *International Conference on Machine Learning*. PMLR, 38087–38099.
- [37] Yuzhuang Xu, Xu Han, Zonghan Yang, Shuo Wang, Qingfu Zhu, Zhiyuan Liu, Weidong Liu, and Wanxiang Che. 2024. OneBit: Towards Extremely Low-bit Large Language Models. *arXiv preprint arXiv:2402.11295* (2024).
- [38] Dongqing Zhang, Jiaolong Yang, Dongqiangzi Ye, and Gang Hua. 2018. Lq-nets: Learned quantization for highly accurate and compact deep neural networks. In *Proceedings of the European conference on computer vision (ECCV)*. 365–382.
- [39] Kaiyong Zhao and Xiaowen Chu. 2014. G-BLASTN: accelerating nucleotide alignment by graphics processors. *Bioinformatics* 30, 10 (2014), 1384–1391.
- [40] Shuchang Zhou, Yuxin Wu, Zekun Ni, Xinyu Zhou, He Wen, and Yuheng Zou. 2016. Dorefa-net: Training low bitwidth convolutional neural networks with low bitwidth gradients. *arXiv preprint arXiv:1606.06160* (2016).